J. Fluid Mech. (1965), *vol.* 21, *part* 1, *pp.* 145–172
Printed in Great Britain

On the behaviour of small disturbances to Poiseuille flow in a circular pipe

By A. E. GILL

Department of Applied Mathematics and Theoretical Physics,
University of Cambridge

(Received 12 May 1964)

A mathematical analysis of the behaviour of small disturbances to Poiseuille flow in a circular pipe can be tackled in two different ways. In the first of these, the disturbance velocity is expressed as a combination of terms, each of which represents a disturbance of a fixed wavelength that decays with time. In the second approach, each term which contributes to the disturbance velocity represents a disturbance of a fixed frequency that decays with downstream distance. The latter method is given more prominence in this paper, since, in experiments in which disturbances are introduced into the flow in a controlled manner, a constant frequency-generating device is commonly used.

In the main, it is assumed not only that the Reynolds number of the Poiseuille flow is large, but that the frequency, f, of the disturbance is large compared with the frequency, ν/a^2, where a is the radius of the pipe and ν the kinematic viscosity of the fluid. The mathematical problem is then of the singular perturbation type, and the disturbances with the smallest damping rates are confined to thin layers. A simple, but crude, analysis shows among other things that the radius at which the disturbance velocity is a maximum is roughly that at which the velocity of the Poiseuille flow is equal to the frequency, f, times the disturbance wavelength. Eigenfunctions are found precisely for the two limiting cases in which, as fa^2/ν tends to infinity, the disturbance becomes confined to a thin layer situated (a) near the centre of the pipe, and (b) near the wall. The eigenfunctions are presented graphically in such a way that immediate comparison can be made with some of Leite's experimental results. Good agreement is found. A real disturbance, however, is made up of several modes, each of which is damped at a different rate with increasing downstream distance. Possible changes in the form and apparent damping rate of a disturbance are discussed in terms of a particular case.

Next, an asymptotic procedure is carried out, which proves to give a good approximation to the eigenvalues and eigenfunctions over a wide range of conditions. From the eigenvalue equation so obtained it is possible to calculate the wave-speed and damping rate for each mode as a function of the non-dimensional frequency, fa^2/ν, and the Reynolds number. For simplicity, the calculations are carried out for the case in which the Reynolds number is infinite, so that the eigenvalues depend only on fa^2/ν. For each mode it is found that the damping rate is an increasing function of the frequency for high frequencies, but as the frequency is decreased the damping rate approaches a limiting value.

These limiting values can be quite small for the Reynolds numbers, R, at which experiments are normally carried out, and for some low-frequency disturbances the distance required for the disturbance amplitude to be reduced by half is as much as $R/100$ diameters.

1. Introduction

Historical development

This paper is concerned with the stability to small disturbances of Poiseuille flow in a pipe, a problem that has been of as great an interest as it has been elusive in its solution since the classical experiments of Osborne Reynolds (1883), which showed that flow in a pipe can become unsteady when the Reynolds number exceeds a certain value, of about 2000. This result prompted Rayleigh (1880) to begin a series of theoretical investigations into the stability to small disturbances of various fluid flows. Rayleigh (1892) thought at first that the mechanism of the observed instability must be primarily an inviscid one, the flow being stable at smaller Reynolds numbers only in consequence of the steadying effect of viscosity. However, his analysis for inviscid fluids led to the conclusion that the flow is *not* unstable, thus creating something of a paradox. Kelvin's (1887) resolution for some related problems was to support Reynolds's (1883) 'idea that the condition might be one of instability for disturbances of a certain magnitude, and stable for smaller disturbances'. Rayleigh (1892) himself suggested that inviscid theory might be inapplicable; for instance, the condition that there is finite slip at the walls is violated no matter how small is the viscosity. Subsequent work (Lin 1955, ch. 3) has shown that Rayleigh's idea explains the instability of *plane* Poiseuille flow, but further experiments by Taylor (unpublished), Ekman (1910) and others for flow in a circular pipe have shown that, by taking sufficient care with entry conditions, the onset of instability can be delayed to very high Reynolds numbers (40,000 and more), which seems to support the finite amplitude explanation for instability in the pipe. The theoretical work that has been done supports this idea insofar as only stable solutions have been found.

Sexl (1927) appears to be the first to take account of viscosity in this problem, in considering the stability of axisymmetric disturbances. However, for reasons of mathematical simplicity, he applied some artificial boundary conditions, so that no reliance can be made on his conclusions. Pretsch (1941) noted that if the disturbance is confined to a thin layer near the wall of the pipe, the problem becomes identical with that of disturbances near the wall in plane Couette flow. Pekeris (1948) found a different set of solutions for which the disturbance was mainly confined to a thin region near the centre of the pipe. Corcos & Sellars (1959) took account of both the limiting class of solutions found by Pekeris, and the class of solutions indicated by Pretsch. However, on this basis they reached the conclusion that only a finite number of eigenfunctions exist, which would imply that the normal mode method so frequently used in stability problems is inadequate for this case, for how can an arbitrary initial disturbance be represented in terms of a finite number of eigenfunctions? Schensted (1960) has since resolved the problem and shown that, in the case of axisymmetric disturbances, not only

does an infinite set of eigenfunctions exist but the set is complete. This paper will be concerned primarily with the calculation of eigenvalues and eigenfunctions so that comparison can be made with experiment.

The type of problem considered

It is desired in this paper to compare theoretical predictions about the behaviour of small disturbances to Poiseuille flow in a pipe with the results of suitable experiments. To find how a disturbance behaves, one needs to know sufficient boundary and initial conditions to specify the solution of the disturbance equations uniquely in the region of interest. In many experiments, disturbances are introduced into the flow in a rather random and unknown way so that little can be said about their behaviour. Obviously, experiments in which disturbances are introduced into the flow in a specified way will be more useful for comparison purposes. Such experiments have been carried out by Leite (1956, 1959) in conjunction with the theoretical work of Corcos & Sellars (1959). Since sinusoidally varying disturbances are usually considered in mathematical treatments of the problem, the disturbances were generated by a mechanism the electrical input into which had a sinusoidal variation with time. After a while, the transients produced by starting the disturbance generating device die away, and the components of the disturbance velocity at any point then vary sinusoidally with time also, and with the same frequency as the input into the generating device. This paper will be concerned with the properties of such disturbances.

The corresponding mathematical problem can be expressed as follows. Let (x, r, θ) be cylindrical polar co-ordinates such that $r = 0$ represents the centre-line of the pipe and x increases in the downstream direction, and let t be the time. For time $t < 0$ we suppose that the Poiseuille flow is undisturbed, and that at $t = 0$ a disturbance generating device comes into operation in a certain finite region. This may be regarded as equivalent to a force which is equal to the real part of

$$f(x, r, \theta)\, e^{-i\omega t},$$

where f is a generalized function, zero outside a certain finite region. The problem is to find the disturbance velocity produced in this way for times large enough for the transients to have died away.

Representation of the disturbance velocity

(i) *θ-dependence.* The disturbance velocity can be expressed as a Fourier series in θ of the form

$$\mathbf{u}(x, r, \theta, t) = \sum_{n=-\infty}^{\infty} \mathbf{u}_n(x, r, t)\, e^{in\theta}.$$

The equations being linear, each term of the series can be considered separately, and the equations for each $\mathbf{u}_n(x, r, t)$ will not involve θ explicitly.

(ii) *(x, r, t)-dependence.* There are two ways which seem appropriate for the representation of $\mathbf{u}_n(x, r, t)$.

(*a*) *The timewise problem.* One method is to express each $\mathbf{u}_n(x, r, t)$ as a Fourier integral over the range of wave-numbers, α, viz.

$$\mathbf{u}_n(x, r, t) = \int_{-\infty}^{\infty} \bar{\mathbf{u}}_n(r, t; \alpha)\, e^{i\alpha x}\, dx.$$

Each $\mathbf{u}_n(r,t;\alpha)$ satisfies differential equations involving only derivatives with respect to r and t and the following conditions are sufficient to determine $\bar{\mathbf{u}}_n$ for all $t > 0$: that $\bar{\mathbf{u}}_n$ vanishes on the walls of the pipe, and that the initial value of $\bar{\mathbf{u}}_n$ is given.

One way of solving the equation for $\bar{\mathbf{u}}_n(r,t;\alpha)$ is to take Laplace transforms with respect to time of each side of the equation, and thus find the Laplace transform with respect to time of $\bar{\mathbf{u}}_n$. The function $\bar{\mathbf{u}}_n(r,t;\alpha)$ will then be given by the usual integral for the inverse transform, and this integral is generally found to be equivalent to a sum of residues. Alternatively, the residues correspond to eigenfunctions which can be found directly by looking for solutions of the form

$$\mathbf{u}(x,r,\theta,t) = \mathbf{u}(r)\exp(in\theta + i\alpha x - i\beta t), \tag{1.1}$$

where α is given, β is one of the complex eigenvalues to be determined, and $\mathbf{u}(r)$ vanishes on the wall of the pipe. The problem of looking for these eigenfunctions and eigenvalues will be termed the 'timewise' eigenvalue problem, since the solution corresponding to each eigenvalue represents a disturbance of a given wave-number which grows or decays with time.

Notice that $\mathbf{u}(r)$ is a vector eigenfunction, but, because of the continuity equation, is equivalent to two scalar eigenfunctions rather than three. In the case of axisymmetric disturbances ($n = 0$), the radial and azimuthal components of $\mathbf{u}(r)$ satisfy independent equations and to each of those components corresponds a different set of eigenfunctions. Schensted (1960) has shown that the set corresponding to the radial component is complete.

(*b*) *The spacewise problem.* The method which seems the most useful for comparison with experiment has the known sinusoidal dependence on time built into the solution from the start. The method is suggested by the form of (1.1), which has the required time dependence if β is taken to be equal to the angular frequency ω, of the generating device. Then, for given n, α becomes an eigenvalue to be sought. The problem of looking for eigenvalues and eigenfunctions of this type will be termed the 'spacewise' eigenvalue problem since the solutions corresponding to each eigenfunction represents a disturbance of a fixed frequency which grows or decays with increase of the space variable, x (cf. Watson 1962).

It is important to consider the boundary conditions appropriate to the spacewise problem, particularly since they are a little more complicated than those for the timewise problem. For this purpose, the spacewise problem can be split up into two stages, the first being to write $\mathbf{u}_n$ in the form

$$\mathbf{u}_n(x,r,t) = \exp(-i\omega t)\,\bar{\bar{\mathbf{u}}}_n(x,r;\omega),$$

so that $\bar{\bar{\mathbf{u}}}_n$ satisfies equations involving only derivatives with respect to x and r. These equations are elliptic, and so require for their solution that $\bar{\bar{\mathbf{u}}}_n$ be specified on a *closed* surface, such as the one formed by the wall of the pipe and two bounding cross-sections, $x =$ constant. Allowing the downstream cross-section to approach $x = \infty$, it is seen that the following boundary conditions are appropriate: that $\bar{\bar{\mathbf{u}}}_n$ vanishes on the walls of the pipe, that $\bar{\bar{\mathbf{u}}}_n$ is as specified for a given value of x, and that the behaviour of $\bar{\bar{\mathbf{u}}}_n$ as $x \to \infty$ is consistent with the fact that the disturbance generator is upstream of cross-sections represented by these large values of x.

The last condition represents a complication which does not appear in the timewise problem, and is similar to the radiation condition that is required in many wave-motion problems. The restriction is necessary because disturbances can be propagated upstream as well as downstream, and it is necessary to eliminate those solutions which correspond to disturbances propagating upstream from $x = \infty$. Such disturbances, as one might expect, are quickly damped out, and it is not difficult in practice to decide which solutions have the right behaviour as $x \to \infty$.

The solutions given most attention below, however, are of the singular perturbation type, so that a boundary-layer approximation can be made, the changes with downstream distance being slow compared with the changes across the thin annular layer to which most of the disturbance is confined. As a consequence, the equations become parabolic instead of elliptic and can be treated in much the same way as timewise solutions.

Notice again that $\mathbf{u}(r)$ is a vector eigenfunction. For the spacewise problem it is equivalent to three scalar eigenfunctions, since the continuity equation does not reduce the number of independent components as it does in the timewise problem. This paper will be devoted to finding spacewise eigenfunctions, as they may readily be compared with experimental results. Of these eigenfunctions, the ones of most interest will be those corresponding to the smaller damping rates. Those corresponding to large damping rates will generally be ignored.

2. Equations for a small disturbance to flow in a pipe

Some physical considerations

In discussing the stability of unidirectional flows in two dimensions, it is useful to consider the vorticity associated with certain material lines of fluid (Lin 1955, § 4.4). For the axisymmetric motions we are to consider, the equivalent discussion is that of material rings of fluid, the centres of the rings being on the axis. A given material ring will remain a ring of this type throughout its motion. Such rings coincide with vortex lines, and for motion in an inviscid fluid the vorticity associated with any material ring varies in proportion to its circumference. In other words, the quantity, Z, that is equal to the vorticity associated with the ring divided by its radius, remains constant for a material ring of fluid. Now, the value of Z at any fixed point can be divided into a mean part, $\bar{Z}$, and a fluctuating part, Z_f,

$$Z = \bar{Z} + Z_f,$$

where the bar denotes the mean with respect to time at a fixed point. For sufficiently small disturbances, $\bar{Z}$ can be identified with the value of Z for the basic flow, and this is a function only of r. Thus as the radius of a material ring alters, $\bar{Z}$ will change and so correspondingly Z_f must change in order to keep Z a constant. This represents a mechanism for the exchange of vorticity between the mean flow and the disturbance. The special feature of Poiseuille flow, however, is that $\bar{Z}$ is independent of t, and so this exchange mechanism does not operate for very small disturbances.

In a viscous fluid, the effect of viscosity in the interior of the fluid will be to damp out disturbances. However, there is another interchange mechanism

which operates at the solid boundary in a way that apparently cannot be determined *a priori*. This mechanism corresponds to the fact that the value of Z_f at the wall can change in a viscous fluid, which implies that vorticity can be generated by or absorbed by the wall. It would be very surprising if this effect alone were responsible for instability, as the wall is not a source of energy, and this leads one to suspect that all small disturbances will be stable. However the existence of the exchange mechanism at the wall prevents what would be a simple proof of stability. The same difficulty arises in a paper by Sexl & Spielberg (1958) in which lack of knowledge of the quantity (9) in their paper is equivalent to the lack of knowledge of the amount of vorticity generated by or absorbed by the wall in the above discussion.

Non-dimensional form of the equations

The equations can be put in non-dimensional form by choosing as the respective units of velocity, length and density the maximum velocity, $U_{\max.}$, of the basic flow, the radius, a, of the pipe, and the density, ρ, of the fluid. Then the kinematic viscosity of the fluid can be replaced in the equations by the reciprocal of the Reynolds number, R, defined by

$$R = U_{\max.} a/\nu.$$

The basic Poiseille flow will have cylindrical polar components

$$(1-r^2, \quad 0, \quad 0),$$

and it has been seen that the velocity perturbation can be expressed in terms of particular velocity perturbations of the form (1.1). Let the cylindrical components of $\mathbf{u}(r)$ be $u(r)$, $iv(r)$, $w(r)$, where the factor i is introduced because of the phase difference of $\frac{1}{2}\pi$ between the radial component and the other components, which follows from the continuity equation.

Attention will be restricted to axisymmetric disturbances ($n = 0$), because such disturbances are simpler to handle theoretically while showing many of the features of more general disturbances, and the disturbances generated in Leite's experiments were mainly axisymmetric. The simplifying feature in the case of axisymmetric disturbances is that the sixth-order set of equations satisfied by the velocity components can be divided into two independent sets of equations, one set being of the fourth order and the other of the second. The second-order equation, which involves only the azimuthal component, w, of the velocity is

$$[\alpha R(1-r^2) - \beta R]w = -i(w'' + w'/r - \alpha^2 w).$$

The behaviour of this component follows very simply from the analysis to follow, since w satisfies an equation very similar to (2.4) below. For the purpose of studying the other components, however, w can be taken to be zero, and this will be assumed in most of the following discussion. The fourth-order set of equations involves only the axial and radial components of disturbance velocity, and these components can be expressed in terms of a disturbance stream function. For an eigenmode, this will have the form

$$\phi(r)\, e^{i\alpha x - i\beta t}, \tag{2.1}$$

and the components u and v will be given by

$$u = \phi'/r, \quad v = -\alpha\phi/r. \tag{2.2}$$

The fluctuating part, Z_f, of Z will have the corresponding form

$$\zeta(r)\, e^{i\alpha x - i\beta t},$$

where

$$r^2\zeta = -(\phi'' - \phi'/r - \alpha^2\phi). \tag{2.3}$$

The equation satisfied by ζ (given in a different form by Sexl 1927) is

$$[\alpha R(1-r^2) - \beta R]\,\zeta = -i(\zeta'' + 3\zeta'/r - \alpha^2\zeta), \tag{2.4}$$

and the four boundary conditions are (i) that there is no source of fluid on the axis, that is $\phi = 0$ at $r = 0$ (this is equivalent to two conditions); (ii) that the velocity vanishes at the wall, i.e. $u = v = 0$ at $r = 1$.

For given α, the solutions of the above equation satisfying the above boundary conditions are timewise eigenfunctions with corresponding eigenvalues, β. For given β, the solutions of the above equation satisfying the above boundary conditions are spacewise eigenfunctions with corresponding eigenvalues, α. In the latter case, however, there is also a condition on α required to give the correct behaviour as $x \to \infty$.

The function ϕ does not appear explicitly in (2.4) because of the lack of the vorticity exchange mechanism discussed previously. Notice also that, as in other problems for which there is an imposed frequency or length scale, the relative importance of the viscous terms is not represented by the Reynolds number alone, but through the parameter βR in the case of an imposed frequency, and through the parameter αR in the case of an imposed axial length scale. If the imposed frequency is f, then βR is described in terms of dimensional quantities by the relation

$$\beta R = 2\pi f \alpha^2/\nu,$$

and so measures the imposed frequency in relation to the quantity α^2/ν, which has the dimensions of frequency.

3. General discussion of the types of solution

Inviscid solutions of the spacewise problem

If the effect of viscosity is small throughout the fluid, equation (2.4) reduces to the inviscid equation, $\zeta = 0$, or by (2.3)

$$\phi'' - \phi'/r - \alpha^2\phi = 0,$$

and the boundary condition to be applied at the wall is that of no flux across the wall, namely

$$\phi(1) = 0.$$

The regularity condition to be applied at the centre can be written

$$\phi(0) = 0.$$

For the timewise problem where α is real and given, there are no solutions to the inviscid problem, but in the spacewise problem where α is a complex eigenvalue to be found, there is a complete (scalar) set of solutions with α such as to give an appropriate behaviour for $x \to \infty$. These solutions are given by

$$\phi = rJ_1(\sigma_m r), \quad \alpha = i\sigma_m, \quad \text{where} \quad m = 1, 2, 3, \ldots,$$

σ_m being the zeros of $J_1(\sigma)$, that is

$$J_1(\sigma_m) = 0.$$

These solutions will not be considered further since the least damped of the disturbances represented here suffers a loss of amplitude by a factor of 2000 in a downstream distance of one diameter.

It is worthwhile, however, to take stock of the number of eigenvalues found, and the number yet to be found. It has already been remarked that the set of spacewise vector eigenfunctions is equivalent to three scalar sets of eigenfunctions. For the axisymmetric case, one scalar set corresponds to the azimuthal velocity component, and another scalar set for large values of βR is the set of inviscid solutions just found. This leaves one more set to be found, for large values of βR, and since we have found all the inviscid solutions, the remaining set must be of the singular perturbation type, in which the viscosity is important in some thin layer, or for motion of a small length scale.

For the timewise problem, the set of vector eigenfunctions is equivalent to only two scalar sets of eigenfunctions, since the continuity equation cannot allow the three components of velocity to be chosen independently at a given time. For axisymmetric disturbances, one set corresponds to the azimuthal velocity component and since there are no inviscid solutions, the other set must, for large αR, comprise solutions of the singular perturbation type.

Singular perturbations or 'viscous' solutions

The inviscid solutions correspond to the vorticity being everywhere small. In contradistinction, the 'singular perturbation' or 'viscous' solutions must be such that the vorticity is not small, at least in some part of the flow. In the spacewise problem, for example, the part of the flow in which the vorticity is small could be a thin layer whose width depends on the large parameter, βR, or alternatively, the vorticity could vary rapidly with radius, the variations being on a small length scale dependent on βR.

It is worthwhile at this stage to consider the relation between the position of this layer and the wave-number, α_r, of the disturbance produced. For instance, in some of Leite's experiments, disturbances are produced by oscillations of a circular airfoil, of radius, r_0, say. In that case one would expect that the maximum disturbance not too far downstream of the airfoil is situated close to r_0, and since the stream is sweeping past the airfoil with velocity $U(r_0)$, it is natural to expect the disturbance to have its wave-number, α_r, given by

$$\alpha_r U(r_0) = \beta. \tag{3.1}$$

To put the argument another way round, a singular perturbation type of eigenmode with wave-number α_r can be expected to have the disturbance maximum close to the points, r_0, given by (3.1). In practice, of course, there will be an infinite number of possible modes, and those stimulated the most can be expected to be the ones with maxima close to the radius, r_0, and with wave-numbers α_r that satisfy (3.1) the most closely.

Now let us examine equation (2.4) for the vorticity and see to what extent these ideas are substantiated. Equation (2.4) is a second-order equation

containing a large parameter, and as such the behaviour of its solutions in certain regions of the complex r-plane are well known (Erdélyi 1956, ch. 4). The equation has singularities at two points only; $r = 0$ which is a regular singularity, and $r = \infty$ which is an essential singularity. When, however, the parameter contained in the equation is large, two other points become important. They are called transition or turning points and are the points where the large coefficient of ζ in (2.4) is zero, that is the points are given by $r = \pm r_c$, where

$$r_c^2 = 1 - \beta/\alpha. \tag{3.2}$$

If we define r_c as the root which has positive real part, it is only the transition point at $r = +r_c$ that need concern us. In hydrodynamic stability problems it is usually referred to as the critical point, and we will use this name for the single point r_c. It should be noted in passing that if $|\alpha|$ is comparable to R, the critical point will not be at the position given by (3.2) since the coefficient, $i\alpha^2$, of ζ on the right-hand side of (2.4) is as important as those on the left-hand side. If this term is included we find that

$$r_c^2 = 1 - \beta/\alpha - i\alpha/R.$$

Disturbances of such large wave-number, however, are damped out very rapidly indeed, so are not of great physical interest and will be ignored.

Certain asymptotic approximations to solutions of (2.4) are well known (Erdélyi 1956, ch. 4). They are given by

$$\zeta \sim (r^3 g')^{-\frac{1}{2}} e^{+ig}, \tag{3.3}$$

where

$$g'^2 = i\beta R - i\alpha R(1 - r^2) \tag{3.4}$$

and $-\frac{1}{2}\pi < \arg g' \leqslant \frac{1}{2}\pi$, and are valid in certain regions away from the singular points and the transition points. For instance, it is assumed that $|g'|$ is large, which requires that r should not be too close to r_c. Now, from the physical point of view, it is the behaviour of the solutions for r real and such that $0 \leqslant r \leqslant 1$ that matters, so let us see how the approximations (3.3) behave for this range of r. Since g' is large in magnitude, ζ can be expected to vary rapidly with r, and so also will $|\zeta|$ except where g' is approximately real. The point, r_m, where g' is real, is important, as it marks a maximum or minimum of $|\zeta|$. By the definition (3.4) of g', the point r_m is given by

$$r_m^2 = 1 - \beta/\alpha_r, \tag{3.5}$$

α_r being the real part of α. This formula is in fact identical for Poiseuille flow with the formula (3.1) which gives the point where the disturbance might be thought to be a maximum on physical grounds. Note also that the imaginary part of (3.4) shows that

$$\alpha_i R(1 - r_m^2) = g'^2, \tag{3.6}$$

and so α_i is positive, g' being real at the point r_m. This means that these solutions with a local maximum of $|\zeta|$ are damped, as can be expected from the 'physical considerations' of § 2 when boundary values have no effect in determining the solution. In fact, given that at any cross-section $|\zeta|$ has a maximum value at a certain radius, one would expect vorticity to be diffused radially away from the maximum, this leading to a reduction in its magnitude with increasing distance from the source of the disturbance.

Now there are a number of conditions that need to be fulfilled for (3.3) to be a valid approximation near $r = r_m$. One is that r_m should not be too close to $r = 0$, which is a singularity of the equation, and another is that r_m should not be too close to the boundary $r = 1$ where boundary conditions will be important and also since, by (3.6), g' will be small at $r = r_m$. These two cases will be examined in detail in §§ 4 and 5. Another condition which should be satisfied is that g' should be large at $r = r_m$, that is that r_m should not be too close to the zero r_c of g'. In practice, it is found that, under the conditions of Leite's experiments at least, r_m is too close to r_c for (3.3) to be a very good approximation at that point, but is far enough away for (3.5) to give a reasonable estimate of the position of the maximum, and to give a good idea of the way ζ varies. For this reason, it is worth examining further the properties of the disturbances that (3.3) represent. The way that this type of approximation to the solution should be modified near the critical point will be discussed in § 6.

Behaviour of the disturbance velocity near $r = r_m$

The disturbance velocity components corresponding to the vorticity given by (3.3) can be found by integration. First, ϕ can be found by using (2.3), which gives to the first order

$$\phi = r^{\frac{1}{2}} g'^{-\frac{5}{2}} e^{ig} + \text{an inviscid solution}. \tag{3.7}$$

The inviscid part of the solution varies slowly compared with the viscous part, and will be determined by boundary conditions applied at points where we have assumed that the viscous part is relatively small. This means that the inviscid part of the solution will be relatively unimportant in the layer to which the disturbance is mainly confined, and so can be ignored there. Thus (2.2) gives

$$u = \phi'/r \approx i r^{-\frac{1}{2}} g'^{-\frac{3}{2}} e^{ig}, \tag{3.8}$$

and $|u|$ is also a maximum near $r = r_m$.

To find how u changes near $r = r_m$, g and g' can be expanded as power series in

$$y = r - r_m.$$

For sufficiently small y, this gives

$$u = u_m(1 - \ldots) \exp\{i[\alpha_i R(1 - r_m^2)]^{\frac{1}{2}} y - \alpha_r R r_m [\alpha_i R(1 - r_m^2)]^{-\frac{1}{2}} y^2/2 + \ldots\}. \tag{3.9}$$

which indicates the rapid phase changes across the layer and the sharp peak in the amplitude.

It is clear that the above analysis can give no estimate of the eigenvalues since no account is taken of the boundary conditions, but if a_r and a_i are measured experimentally, the approximation (3.8) and (3.9) give an estimate of the disturbance velocity variations. This allows a comparison to be made with Leite's experimental results. For the measurements made at the station closest to the disturbance generator it is found that (3.5) is only in error by about 5 % for disturbances generated by the sleeve, and the estimates of the width of the layer and of the rate of change of phase at $r = r_m$ given by (3.9) are, rather surprisingly in the light of the crudity of the assumptions made, usually found to be in error

by less than 30 %. Hence the above analysis seems to be a useful guide, even though it cannot be expected to be very accurate. In § 6, a more complete analysis will be carried out taking account of the boundary conditions and of the different approximations that are valid in different parts of the complex r-plane. In the next two sections, the two special cases will be examined in which the layer is close to the centre of the pipe or close to the wall.

4. Analysis for disturbances confined to a thin region near the centre

For disturbances of the singular perturbation type which are confined to a thin region near the centre of the pipe, the non-dimensional wave-number α_r will be approximately equal to β, as (3.5) indicates when r_m is close to zero. The thickness of the layer to which disturbances are confined will be determined by a balance between convection processes and viscous processes. To understand a little more of these processes, it is instructive to consider what would happen to a disturbance of fixed wave-number in an inviscid fluid, where Z_f is changed only by convection. If initially, neighbouring radial points are in phase, then they will become more and more out of phase as time goes on due to the shearing motion, which changes the phase at different radii at different rates. For instance if the initial value of Z_f defined in § 2 is equal to $\cos(\alpha_r x)$, the value of Z_f at time t will be

$$Z_f = \cos\{\alpha_r[x - U(r)t]\},$$

and differentiation of this expression with respect to r shows how the radial gradients grow with time. The same is true at large times if the initial value of Z_f has the form $f(r)\cos(\alpha_r x)$. In a real fluid, of course, gradients cannot steepen indefinitely, as viscous diffusion will tend to smooth out the steep gradients, at the same time damping the disturbance.

Near the centre of the pipe the shearing motion is not very pronounced and so the effects discussed above will be relatively weak. It turns out, in fact, that disturbances with maxima nearer the centre have smaller rates of damping. The thickness of the layer, the rate of damping, etc., can be estimated in order of magnitude as follows. In dimensional terms, if l is the thickness of the layer, the shear is of order $U''l$ and the rate of change of ζ due to convection at one point in the layer is of order $\alpha_r U''l^2\zeta$ relative to the rate at another point in the layer. The rate of change due to diffusion, on the other hand, is of order $(\nu/l^2)\zeta$ and the two effects balance in a layer of thickness

$$l \sim (\nu/\alpha_r U'')^{\frac{1}{3}}.$$

Thus the greater the shear gradient, the thinner the layer, and the greater the viscosity the more the layer is spread out. The time rate of damping of the disturbance is of order $(\nu/l^2)\zeta$, so that the spatial rate is given by

$$\alpha_i U \sim \nu/l^2 \sim (\nu\alpha_r U'')^{\frac{1}{3}}.$$

In non-dimensional terms

$$l \sim (\alpha_r R)^{-\frac{1}{3}} \sim (\beta R)^{-\frac{1}{3}}$$

and

$$\alpha_i R \sim (\alpha_r R)^{\frac{1}{3}} \sim (\beta R)^{\frac{1}{3}}.$$

There is little difference between the timewise and spacewise problems in this limit, as a spatially decaying disturbance can also be regarded as a time-decaying disturbance being convected with the fluid at the centre of the pipe. Also, since α_i/α_r is small, α and β are approximately the same, and the analysis to follow applies equally well to the timewise and spacewise problems.

This limiting problem has been considered previously by Pekeris (1948), who found a simple formula for the eigenvalues. Corcos & Sellars (1959) found the same formula, but by a method that seems open to question. Gill (1962) later indicated that the eigenfunctions can also be expressed in a simple form. They are calculated as follows. Taking note of the above scalings, a new radial variable s can be defined by

$$s = e^{-\frac{1}{4}i\pi}(\alpha R)^{\frac{1}{2}}r^2. \tag{4.1}$$

The factor $\exp(-\frac{1}{4}i\pi)$ is included here and in the following definition so that the resulting equation will not contain 'i' explicitly. The constant coefficient of ζ in (2.4) can be collected together and scaled as follows:

$$i\beta R - i\alpha R - \alpha^2 = 4e^{-\frac{1}{4}i\pi}(\alpha R)^{\frac{1}{2}}m, \tag{4.2}$$

so that (2.4) becomes

$$4s\,d^2\zeta/ds^2 + 8\,d\zeta/ds + (4m-s)\,\zeta = 0.$$

By (4.1), the boundary point $r = 1$ becomes a boundary at $s = \infty$, and so one of the boundary conditions that must be applied to the solutions of the above equation is that $\zeta \to 0$ as $s \to \infty$. ζ in fact has an exponential singularity at ∞, which can be removed by defining

$$\zeta = \eta\, e^{-\frac{1}{2}s}, \tag{4.3}$$

giving in place of the equation for ζ

$$s\,d^2\eta/ds^2 + (2-s)\,d\eta/ds + (m-1)\,\eta = 0.$$

The problem has now become a classical eigenvalue problem: to find the values of m for which the above equation has solutions regular at $s = 0$ and for which $\zeta = \eta\, e^{-\frac{1}{2}s}$ tends to zero as $s \to \infty$. The eigenvalues are the positive integers

$$m = 1, 2, 3, \ldots,$$

and the eigenfunctions are Laguerre polynomials

$$\eta = L^1_{m-1}(s). \tag{4.4}$$

Expressions for the damping rate and wave-speed, c, can be found from (4.2). For the spacewise problem, β is real, and if β is small compared with $R^{\frac{1}{3}}$, we have to the second order

$$c = \beta/\alpha_r = \{1 + 4m(2\beta R)^{-\frac{1}{2}}\}^{-1} \tag{4.5}$$

and to the same order

$$\alpha_i R = 2m(2\beta R)^{\frac{1}{2}} + 8m^2. \tag{4.6}$$

For a given frequency and given Reynolds number, the mode with the least damping is the one given by $m = 1$. This is also the one with largest wave-speed and has maximum $|\zeta|$ at the centre. If the frequency is allowed to vary at a given Reynolds number, the damping rate decreases as the frequency increases, but the decrease is not without limit for when βR is of order unity, the wall is

not outside the layer and the approximation breaks down. The changes at this breakdown will be examined in § 6. If the frequency is increased, (4.5) and (4.6) eventually cease to be valid approximations to (4.2), and if the changes are followed it is found that for very large β, α_r and α_i both asymptote to the values $(\frac{1}{2}\beta R)^{\frac{1}{3}}$. Because of the large damping rate, however, such solutions are of little physical interest. It may also be noted that for β sufficiently large, (4.2) also has solutions for which α_r and α_i are both negative. $-\alpha_i$ is very large, and these represent upstream-moving rapidly damped solutions which are excluded from the permissible set of eigenvalues by the condition for $x \to \infty$.

Disturbance velocity profiles

It so happens that the eigenvalues were found above without reference to disturbance velocities, this being possible due to the remoteness of the solid boundary. The velocity components can be found by integration. For instance, provided that β is small compared with $R^{\frac{1}{3}}$, (2.2), (2.3) and the definition (4.1) of s show that, within the layer, the axial component can be determined by the formula

$$du/ds = \text{const.}\,\zeta = \text{const.}\,\eta\, e^{-\frac{1}{2}s}.$$

η is one of the polynomials (4.4) of degree $(m-1)$, and integration shows that $u\, e^{\frac{1}{2}s}$ is a polynomial of the same degree. The first four modes are represented below, the arbitrary multiplicative constant being omitted:

$$\left.\begin{aligned} m &= 1, \quad u = e^{-\frac{1}{2}s}; \\ m &= 2, \quad u = s\, e^{-\frac{1}{2}s}; \\ m &= 3, \quad u = (1 - s + \tfrac{1}{2}s^2)\, e^{-\frac{1}{2}s}; \\ m &= 4, \quad u = s(6 - 3s + \tfrac{1}{2}s^2)\, e^{-\frac{1}{2}s}. \end{aligned}\right\} \tag{4.7}$$

Actually, there is also an additive constant arising from the integration. Its value, however, is determined by the conditions at the solid boundary, and is small whenever β is small compared with $R^{\frac{1}{3}}$.

The velocity profiles represented by (4.7) are given in terms of their amplitude and phase in figure 1. The value of βR was taken to be 3900 so that direct comparison can be made with Leite's (1956) measurements for that value of βR, reproduced in figure 2. The vertical scales are chosen for easy comparison with Leite's results. Below each curve for the amplitude is shown the extent to which each mode would be damped at the second downstream station according to the theory. The table above the phase curves shows the phase shift that would be expected between the first and second downstream stations according to the theory. Before comparing the two figures, it should be noted that (3.5) gives quite a good estimate of the position of maximum amplitude for modes 3 and 4, though not for modes 1 and 2. Also, the rates of change of phase at the positions of maximum amplitude, and the width of the peaks in the amplitude curves are predicted surprisingly well by (3.9).

Now comparing the two figures, it will be observed that the experimental amplitude curve corresponds very well with the theoretical one for the mode $m = 4$. Also the slope of the experimental phase curve agrees very well with the

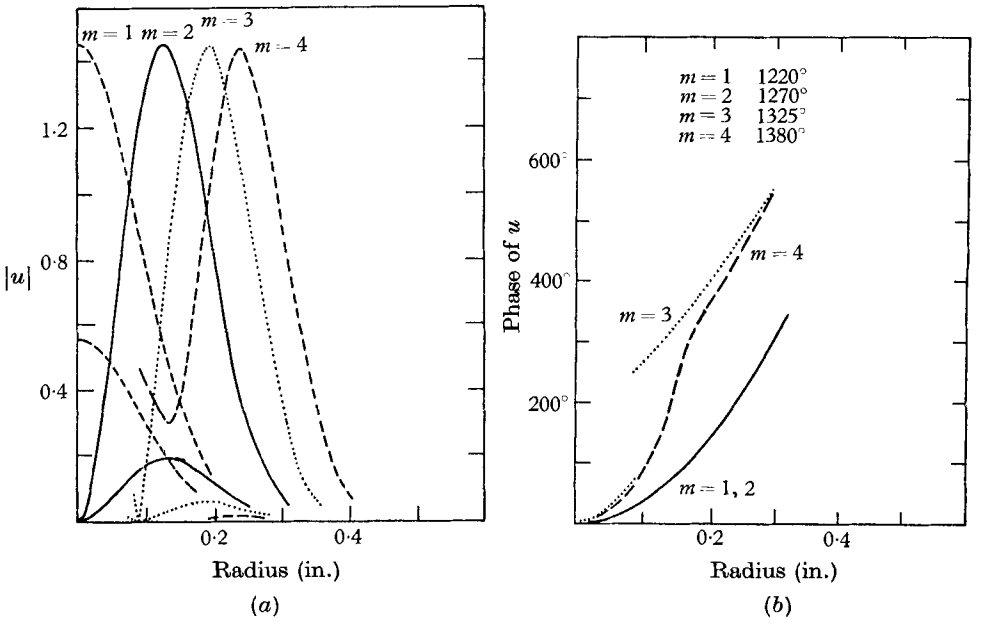

FIGURE 1. Theoretical variation of (*a*) amplitude and (*b*) phase of the disturbance velocity for the modes $m = 1, 2, 3, 4$, with scales appropriate to the conditions stated on figure 2. For each mode a second curve of smaller amplitude is drawn in (*a*) to show the theoretical damping in 10·4 diameters downstream distance (cf. figure 2) and the table in (*b*) shows the theoretical change of phase in the same distance. Part of the curves for $m = 3, 4$ have been omitted to avoid confusion with other curves.

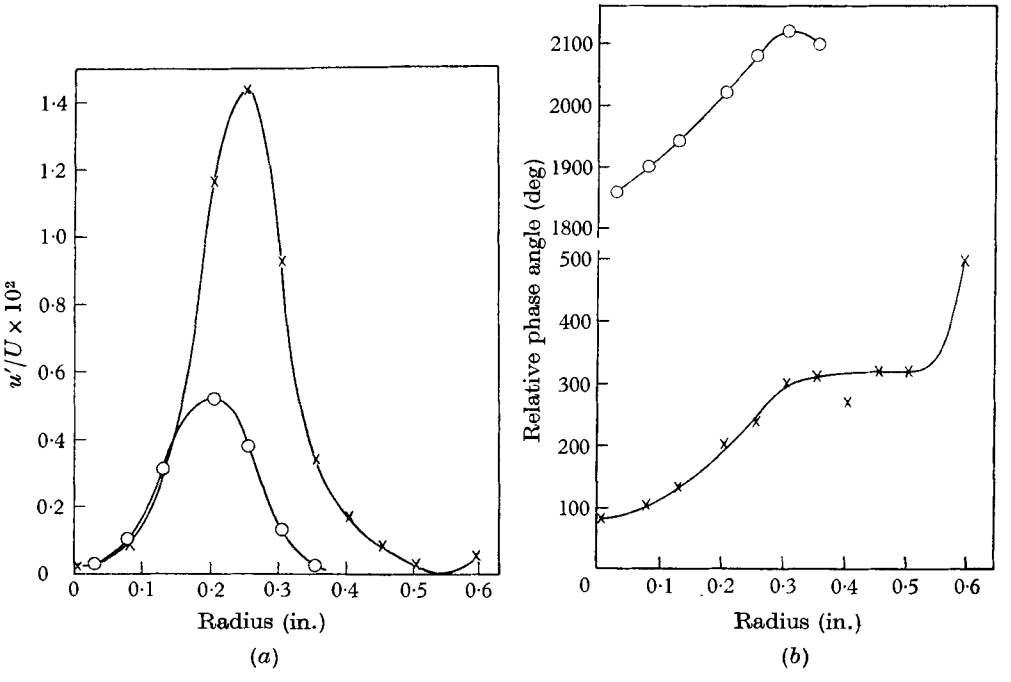

FIGURE 2. Experimental variation of (*a*) amplitude and (*b*) phase of the disturbance velocity, reproduced from Leite (1956). $R = 4000$; $f = 40$ c/s; ×, 18·2 diam. downstream from aerofoil; ○, 28·6 diam. downstream from aerofoil.

slope of the theoretical one at the same point. However, the agreement is not so good for the changes observed with downstream distance: the observed damping is much less than the theory predicts, and the phase shift of 1840° predicted. Also the position of maximum amplitude has shifted nearly to that for the mode $m = 3$. There are three effects which could contribute to such discrepancies:

(1) Non-linear effects may be important under the experimental conditions since Leite found that by feeding more energy into the disturbance generator at the same Reynolds number, growing disturbances could be produced.

(2) It has been assumed that the disturbances are axisymmetric, whereas the disturbance could well be three-dimensional.

(3) The comparison has been made with results for a single mode. This is allowable if one mode is dominant, but it could well be that the disturbance contains two or three modes in comparable amounts. We will therefore consider the behaviour of a disturbance comprising two modes.

A disturbance comprising two modes

Before looking at the particular case of a two-mode disturbance, there are some general remarks that can be made about the sum of an arbitrary number of modes of the type (4.7). First, there is a great variety of possible radial distributions of axial velocity at a particular downstream station, since a combination of modes of the type (4.7) can make $u e^{\frac{1}{2}s}$ equal to an arbitrary polynomial in s. Secondly, the following changes occur in the properties of the modes of the type (4.7) as m increases, assuming that β is small compared with $R^{\frac{1}{3}}$: the damping rate increases (by 4.6); the wave-number increases (by 4.5); and figure 1 shows that for the first four modes at least, the radius at which the amplitude of the disturbance velocity is a maximum increases. Consequently, for a disturbance comprising several such modes, it will be found that with increasing downstream distance the modes corresponding to smaller values of m will become more important, so that the radius at which the maximum disturbance amplitude occurs will tend to decrease, and the rate at which the phase changes with downstream distance will tend to decrease.

Now consider the special case where the disturbance is a linear combination of the two modes $m = 1$ and $m = 2$. As figure 1 shows, these two modes have the same phase variations with radius, so that it is possible for the two modes to reinforce each other in such a way that the amplitude of the combination is equal to the sum of the amplitudes of the two components. On the other hand, the two modes can be completely out of phase, in which case the amplitude of the combination is equal to the difference between the amplitudes of the two component modes. Hence there can be a considerable variety of distributions of amplitude with radius, the differences being due merely to different phase relationships between the two components.

In the case where the two components are out of phase, the resultant amplitude curve will have a zero at a certain radius, r_0, with a corresponding jump in phase of 180°, similar to the one that occurs for the mode $m = 3$ (see figure 1). Leite (1959, p. 81) in fact found such phase jumps for several observed velocity distributions. Notice also that if the two modes have such a phase relationship, or one

close to it, the curve showing the radial change of amplitude will have two maxima—and this is another feature of many of the curves found experimentally. Of course, the zero in amplitude can only occur at a certain axial position, $x = x_0$ say, since the phase relationship between the two modes changes with x. Consequently, an axial traverse at radius $r = r_0$ will show the disturbance amplitude decreasing to zero at $x = x_0$, and then increasing temporarily as x increases further. Also the phase changes found on such an axial traverse would be quite different at the radius $r = r_0 - \delta$ from the change at the radius $r = r_0 + \delta$ because of the phase jump of 180°. This fact highlights the dangers inherent in trying to deduce the damping rate and wave-speed from an axial traverse at only one radial position. Leite, in fact, shows some of the differences between the values of the wave-speed found from axial traverses at different radii in figures 39 to 41 of his 1956 report.

The number of modes of the type (4.7) *for given* βR

It has already been observed that as m increases, the radius, r_m, at which the disturbance amplitude is a maximum increases. For m sufficiently large, r_m will be of order unity and it will no longer be possible to disregard the boundary conditions at the wall, so that the approximation will break down. In effect, this puts a limit on the number of modes of the type (4.7) that exist for a given large βR. To estimate this number, (3.5) can be used as a sufficiently accurate estimate of r_m, and (4.5) shows that r_m becomes of order unity when m is of order $(\beta R)^{\frac{1}{2}}$. In other words, the number of modes of the type (4.7) that exist is of order $(\beta R)^{\frac{1}{2}}$. Since this represents only a finite number, there must exist other 'viscous' modes in order to make up a complete set. In the next section, further modes are found, but again their number is finite. The further modes required are found in § 6.

5. Analysis for disturbances confined to a thin region near the wall

If the disturbance is confined to a thin layer close to the wall, then on the length scale of the disturbances the wall appears to be flat and the undisturbed flow one of uniform shear. These disturbances, then, will be the same as disturbances to plane Couette flow which are confined to a thin layer close to one of the bounding walls. This fact was noticed by Pretsch (1941), and allows us to draw on results obtained for plane Couette flow. Four recent papers on that subject which are relevant are by Zondek & Thomas (1953), Wasow (1953), Grohne (1954) and Riis (1962). However, these authors all adopt the classical approach of seeking the decay or growth with time of disturbances of a given wavelength, rather than the decay or growth with downstream distance of a disturbance of a given frequency. The distinction between the two cases is a real one, for the effect of the wall is important and the wave-speed of the disturbances is small. In this paper, emphasis will be given to the second of the two cases.

The orders of magnitude of the width of the layer, damping rate, etc., can be worked out by the same method as was used in the last section, but we cannot be sure in advance that disturbances will be damped because of the unknown

generation or absorption of vorticity by the wall, discussed in § 2. In dimensional terms, if l is the thickness of the layer, the relation (3.1) suggests that β is of the same order as $\alpha_r U'l$. The rate of change of ζ due to convection for one particle in the layer will differ from that of another particle by order $\alpha_r U'l\zeta$, while the rate of change due to viscous diffusion is of order $(\nu/l^2)\zeta$. The two rates balance when

$$l = O\{(\nu/\alpha_r U')^{\frac{1}{3}}\} = O\{(\nu/\beta)^{\frac{1}{2}}\}.$$

The time rate of damping, or of growth, has order of magnitude given by

$$\alpha_i U'l \sim \nu/l^2 \sim \beta,$$

and so is proportional to the frequency, but at a given frequency, the spatial rate of decay (or growth) is least for the greatest viscosities and smallest shears. This seems a strange result at first, but the reason is that greater viscosity or smaller shear makes for a thicker layer, and hence larger wave-speed, so that the spatial damping rate will decrease while the time rate remains steady. In non-dimensional terms,

$$l \sim (\beta R)^{-\frac{1}{2}},$$

$$\alpha_r R \sim \alpha_i R \sim (\beta R)^{\frac{3}{2}}.$$

Compared with the damping rate (4.6) for disturbances confined to a thin region near the centre, the magnitude of the damping rate for these disturbances is very large.

The appropriate equation is obtained by putting $r = 1 - y$ in (2.4) and assuming that y, the distance from the wall, is small. This gives

$$\frac{d^2\zeta}{dy^2} - i\alpha R\left(2y - \frac{\beta}{\alpha} - \frac{i\alpha}{R}\right)\zeta = 0.$$

Taking note of this equation and of the scalings worked out above, it is convenient to define the scaled variable, z, as follows,

$$z = (2i\alpha R)^{\frac{1}{3}}(y - \beta/2\alpha - i\alpha/2R), \tag{5.1}$$

so that the equation becomes

$$d^2\zeta/dz^2 - z\zeta = 0. \tag{5.2}$$

The value of z at the wall, which we can call $-z_q$, is given by

$$z = z_q = -i\beta R/(2i\alpha R)^{\frac{2}{3}} - \{i\alpha/(2R)^{\frac{1}{2}}\}^{\frac{4}{3}}, \tag{5.3}$$

where for definiteness, the one-third root is taken as the one for which

$$-\tfrac{1}{3}\pi < \arg(i\alpha R)^{\frac{1}{3}} \leqslant \tfrac{1}{3}\pi.$$

The suffix q is used because z_q can have a whole sequence of values, corresponding to the eigenvalues of the problem, and q will be used as an index of the eigenvalues.

The solution of (5.2) that vanishes as $y \to \infty$ is

$$\zeta = \text{const.}\,\mathrm{Ai}(z), \tag{5.4}$$

where the Airy function (Miller 1946) notation is used in preference to the more clumsy expression in terms of Hankel functions that is often used. The eigenvalues will be determined by integrating (5.4) to find the disturbance velocity, and then applying the boundary condition that the velocity vanishes at the wall.

Damping rates and wave-speeds

When the wavelength of the disturbance is large compared with the thickness of the layer, that is, by the scalings found above, if $|\alpha|$ is small compared with $R^{\frac{1}{2}}$ or β is small compared with unity, the disturbance velocity in the layer is contained mainly in its axial component, and by (5.1), (2.2) and (2.3), u is given in terms of z by

$$du/dz = \text{const.}\,\zeta.$$

With an appropriate choice of the arbitrary constants in this formula and in (5.4), this gives

$$u = \int_{-z_q}^{z} \mathrm{Ai}\,(z)\,dz. \tag{5.5}$$

But the disturbance velocity must vanish as $y \to \infty$, and so the following eigenvalue equation for z_q is implied:

$$\int_{-z_q}^{\infty} \mathrm{Ai}\,(z)\,dz = 0. \tag{5.6}$$

Notice that if z_q is a root of (5.6), so also is the complex conjugate, z_q^*. We will use the positive integers, q, to describe the roots of (5.6) with positive imaginary part in order of $|z_q|$, and let $z_{-q} = z_q^*$.

Corcos & Sellars (1959) found rough approximations to the first few roots of (5.6) from numerical tables, and checked the first pair on a differential analyser. In the course of computing the disturbance velocity profile given by (5.5), their value was found to be in error by about 1 %, the value correct to four significant figures being

$$z_{\pm 1} = 4{\cdot}263 \exp(\pm 15^\circ 34' i). \tag{5.7}$$

To find the corresponding damping rate and wave-number, (5.3) must be used. For β small this formula may be written

$$\alpha R = \tfrac{1}{2} e^{\frac{1}{4}i\pi} (\beta R/z_q)^{\frac{3}{2}}. \tag{5.8}$$

Substituting from (5.7) it is clear that the first pair of modes correspond to damped disturbances.

Even for the first root, the value of $|z_1|$ is large, so that the asymptotic approximation to (5.6) for large $|z|$, namely

$$-1 + \pi^{-\frac{1}{2}} z_q^{-\frac{3}{4}} \cos(2/3 z_q^{\frac{3}{2}} + \tfrac{1}{4}\pi) = 0, \tag{5.9}$$

is quite a good approximation. The approximate values of z_1 to z_4 given by this formula are

$$\left.\begin{aligned} z_1 &= 4{\cdot}28 \exp(15^\circ 22' i), \quad z_2 = 6{\cdot}94 \exp(8^\circ 5' i), \\ z_3 &= 9{\cdot}18 \exp(3^\circ 31' i), \quad z_4 = 11{\cdot}18 \exp(4^\circ 15' i), \end{aligned}\right\} \tag{5.10}$$

and it is clear that all disturbances of this type are damped. In fact, this type of disturbance where the effect of the wall is important is damped much more heavily than the type of disturbance examined in § 4, where the effect of the wall is not important, as a comparison of (5.8) with (4.6) shows. Note also the measure of agreement between the approximate value of z, given by (5.10) and the more precise value given by (5.7).

If the results (5.10) are substituted in (5.8), it is found that the damping rate decreases as q increases. Also as q increases, it can be expected that since $|z_q|$ increases, the radius at which the disturbance velocity is a maximum will also decrease, so the trend is the same as that found for the modes studied in § 4 and the radius corresponding to the maximum disturbance can be expected to decrease with downstream distance. In Leite's (1956) experiments, this is found to happen in the large majority of cases, but not without fail. Other features discussed at the end of § 4 which may be expected of disturbances comprising several modes apply also to combinations of modes of the type discussed in this paragraph, and indeed are observed. Examples are the double maxima in some of the curves shown in figures 6 and 7 of Leite's 1959 paper.

It should also be mentioned that (5.8) can be used equally well for timewise disturbances with the same values of z_q, provided that α is small compared with $R^{\frac{1}{2}}$. However, if one attempts to convert the results of the spacewise theory into a timewise form, as Leite does with his spacewise experimental results, they will be found to differ by a considerable factor from the results obtained directly from the timewise theory. The relation (5.1) also is different in the two cases implying that the velocity profiles are different. If in the spacewise problem, β is no longer small, or in the timewise problem $\alpha R^{-\frac{1}{2}}$ is no longer small, the values of z_q are not even the same for the two cases. The changes in z_q in such circumstances are reported in my thesis (Gill 1963). Suffice it here to say that the rate of damping gets very large as the frequency or wave-number of the disturbance increases.

A disturbance velocity profile

The velocity profile for the mode $q = 1$ was computed on the Cambridge computer EDSAC 2. The expression for the axial disturbance velocity at a given time and given downstream position is (5.5), with z given by (5.3). The method was to integrate with respect to y from a large value of y, where end values were calculated by asymptotic expressions, to $y = 0$. The Airy function was calculated simultaneously, using the differential equation (5.2). The numerical procedure adopted was the Adams–Bashforth process, using the EDSAC Library subroutine.

The integration was carried out for the first time using the values of z given by Corcos & Sellars. This gave a non-zero value of u at $y = 0$, and so a small correction had to be made to z_1. The integration was carried out again, and the process repeated until the corrections to z_1 were very small. The value of z_1 so obtained is the one given in (5.7). The corresponding velocity profile is plotted in terms of its modulus and phase in figure 3. The value of βR chosen was 2370, so that direct comparison could be made with some of Leite's results, reproduced in figure 4, which correspond to a value of βR approximately that. Note that β has a small value approximately equal to 0·18.

In the amplitude curves shown in figure 3, the maximum for the upper curve has been chosen to be equal to that obtained in Leite's experiment at the first downstream station. The two lower curves indicate the amount that the disturbance would be damped according to theory at the other two downstream stations

of the experiment. The maximum in the experiments is somewhat closer to the centre of the pipe, indicating the presence of modes other than the one given by $q = 1$, also the damping is somewhat less than that for the mode $q = 1$, as is to be expected if other modes are present. The lower of the phase curves in figure 3 corresponds to Leite's first downstream station, and the other curves to the other stations. The change of phase with downstream distance is a little greater

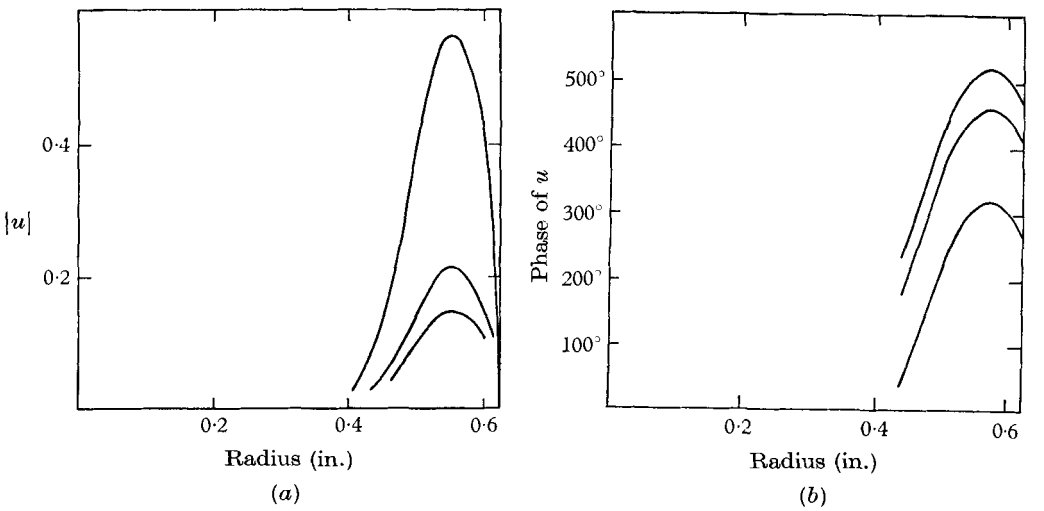

FIGURE 3. Theoretical variation of (*a*) amplitude and (*b*) phase of the disturbance velocity for the mode $q = 1$, with scales appropriate to the conditions stated on figure 4. The curves of smaller amplitude in (*a*) show the theoretical damping in downstream distance of 2·6 and 3·6 diameters (cf. figure 4), while the two upper curves in (*b*) show the theoretical changes of phase in the same distances.

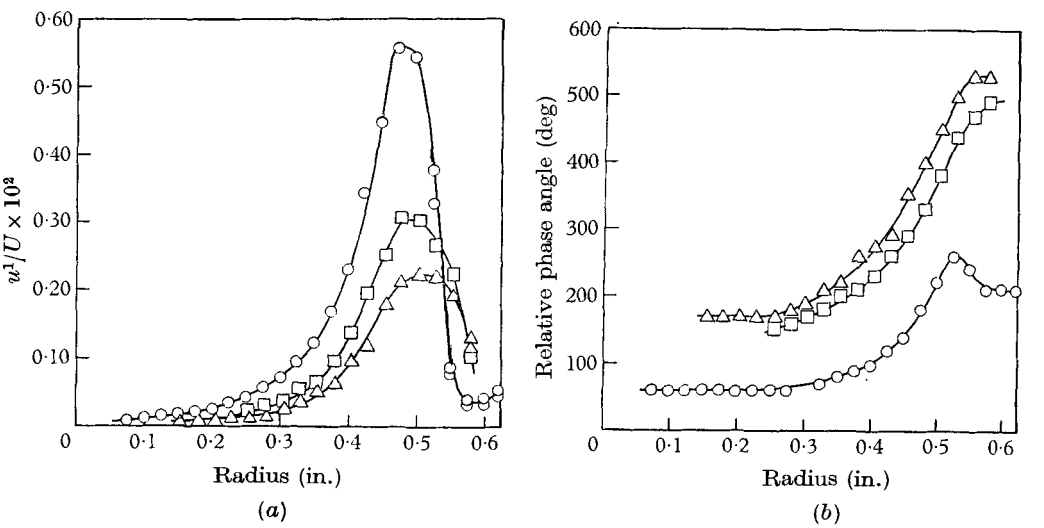

FIGURE 4. Experimental variation of (*a*) amplitude and (*b*) phase of the disturbance velocity, reproduced from Leite (1956). $R = 13{,}000$; $f = 25$ c/s; ○, 3·0 diam. downstream from sleeve; □, 5·6 diam. downstream from sleeve; △, 6·6 diam. downstream from sleeve.

in the experiments than it is for the mode $q = 1$, which is to be expected if other modes are present. Also the rate of change of phase with radius at the radius of maximum amplitude agrees well with the theoretical value. It is also found that the values agree surprisingly well with those expected if the crude formula (3.9) were applied, the errors in position of the maximum being less than 5 % and the errors in the thickness of the layers being of the order of 15 %.

The number of modes of the type (5.5) *for given* βR

As q increases, the position at which the maximum disturbance velocity occurs moves farther and farther away from the wall, and eventually will be at a distance of order unity so that the approximation fails. To estimate the number of modes of the type (5.5) that exist for a given large βR, notice first that for large q, the approximation (5.9) shows that

$$2/3\,|z_q|^{\frac{3}{2}} \sim (2q - 1/4)\,\pi.$$

Using (5.8) for the wave-number and (3.5) to estimate r_m, it will be seen that $(1-r_m)$ is small only if q is small compared with $(\beta R)^{\frac{1}{2}}$. In other words, the number of modes of the type (5.5) that exist is of order $(\beta R)^{\frac{1}{2}}$, and combined with the modes of the type (4.7), the total is still only of order $(\beta R)^{\frac{1}{2}}$. This fact, or the equivalent fact for the timewise problem, caused Corcos & Sellars to reach the conclusion that the number of modes for a given βR is finite. This would be an embarrassment since an arbitrary function cannot be described in terms of a finite number of eigenfunctions, but in the next section a further set of eigenfunctions of the singular perturbation type is found, thus resolving the problem.

6. A comprehensive asymptotic analysis

In § 3, asymptotic approximations, such as (3.3), to solutions of the equations were found. Although these approximations give a rough description of certain features of the flow, their validity is strictly limited and no estimate of the magnitudes of the eigenvalues can be obtained without a more detailed analysis. It is therefore the aim of this section to obtain asymptotic approximations to the eigenfunctions uniformly valid on the interval $0 \leqslant r \leqslant 1$, and to find corresponding approximations to the eigenvalues. The method will be to find approximations valid on different subranges of $0 \leqslant r \leqslant 1$, and to relate the different approximations by standard matching procedures. Approximations of the type (3.3) are valid for part of the interval $0 \leqslant r \leqslant 1$, but break down near the singular point, $r = 0$, and on part of the interval near $r = r_m$ which turns out to be close to the critical point $r = r_c$. Thus four subranges are generally required: a neighbourhood, S_1, of $r = 0$, a subrange, S_2, which lies between $r = 0$ and $r = r_m$, a neighbourhood, S_3, of $r = r_m$, and a subrange, S_4, which covers the rest of the interval up to $r = 1$. The same method can be used to treat the three-dimensional disturbances.

Corcos & Sellars (1959, §§ 4, 5) use a similar method for timewise disturbances, but make use of a procedure which directly connects the approximations valid in S_2 with those valid in S_4. However, in carrying out this procedure they neglect a term which is important in some circumstances, thus leading to the large

discrepancy between the results they find in their § 7 and the more accurate results of their § 9. Hopf (1914) made a similar omission when investigating the stability of plane Couette flow by asymptotic methods, as Riis (1962) pointed out.

First of all, the approximation valid near $r = 0$ can be found from (2.4), which may be written

$$\zeta'' + 3\zeta'/r + \mu^2(1 - r^2/r_c^2)\,\zeta = 0, \tag{6.1}$$

where

$$\mu^2 = i\beta R - i\alpha R - \alpha^2 = -i\alpha R r_c^2. \tag{6.2}$$

For definiteness, we choose the root μ for which

$$-\tfrac{1}{2}\pi < \arg(\mu r_c) < \tfrac{1}{2}\pi.$$

(6.1) has one solution regular at $r = 0$, and for large $(\mu r_c)^2$, this solution is given approximately by

$$\zeta = (\mu r)^{-1} J_1(\mu r),$$

the error being of order $|\mu r_c|^{-2}$ when $|\mu r|$ is of order unity. Integration using (2.3) gives for the stream function, to the same order,

$$\phi = r J_1(\mu r)/\mu(\mu^2 + \alpha^2) + A r I_1(\alpha r), \tag{6.3}$$

A being a constant of integration. This approximation is valid asymptotically for large $|\mu r_c|^2$ provided that $|r/r_c| \ll 1$, so that S_1 can be defined as the range $0 \leqslant r \ll |r_z|$ of values of r. Of the eigenfunctions already found in §§ 4 and 5, the one with the smallest value of $|\mu r_c|^2$ is the mode $m = 1$. By (4.2) and (6.2), the value of $(\mu r_c)^2$ for this mode is 16, which is quite big enough for (6.3) to be a good approximation for this mode, and hence for all modes.

Since we will not be interested in values of $|\alpha|$ as large as $R^{\frac{1}{3}}$, the corresponding disturbances being highly damped, α^2 can be neglected in comparison to μ^2 in (6.3) and for large $|\mu r|$, (6.3) gives approximately

$$\phi = r^{\frac{1}{2}}(2\pi\mu^7)^{-\frac{1}{2}}[\exp\{i(\mu r - \tfrac{3}{4}\pi)\} + \exp\{-i(\mu r - \tfrac{3}{4}\pi)\}] + A r I_1(\alpha r), \tag{6.4}$$

so that the combination of approximations like (3.7) that matches (6.3) is

$$\phi = r^{\frac{1}{2}}(2\pi\mu^2 g'^5)^{-\frac{1}{2}}[\exp\{i(g - \tfrac{3}{4}\pi)\} + \exp\{-i(g - \tfrac{3}{4}\pi)\}] + A r I_1(\alpha r), \tag{6.5}$$

where g' is defined by (3.4) and g is the integral of g' that vanishes at $r = 0$, namely

$$g = \mu \int_0^r (1 - r^2/r_c^2)^{\frac{1}{2}}\, dr. \tag{6.6}$$

The lower 'end' of the range S_2 of the validity of (6.5) is given by $|\mu|\, r \gg 1$, so that S_1 and S_2 have in common the range

$$|\mu|^{-1} \ll r \ll |r_c|,$$

which exists because $|\mu r_c|$ is large. The existence of the overlap range ensures the possibility of matching, the criterion being that (6.5) and (6.6) should have the common asymptotic expression (6.4) in the overlap range.

Now, for all the modes found in §§ 4 and 5, the critical point $r = r_c$ is close in the complex r-plane to the real axis, and since (6.5) breaks down near $r = r_c$,

a new approximation is required for that part of the real axis near the critical point. In any case, the approximation valid near $r = r_c$ can be found by putting

$$r = r_c - y$$

in the equations, and assuming y is small. The approximate equations are, in fact, of the same type as those studied in § 5, although y has been defined slightly differently in this section. For instance, (6.1) becomes

$$\frac{1}{\sigma^2}\frac{d^2\zeta}{dy^2} + \sigma y\zeta = \frac{1}{\sigma r_c}\left[3\left(1-\frac{\sigma y}{\sigma r_c}\right)^{-1}\frac{1}{\sigma}\frac{d\zeta}{dy} - \tfrac{1}{2}(\sigma y)^2\zeta\right], \tag{6.7}$$

where

$$\sigma^3 r_c^3 = 2\mu^2 r_c^2 = -2i\alpha R r_c^4, \tag{6.8}$$

and we choose $-\frac{1}{3}\pi < \arg(\sigma r_c) \leqslant \frac{1}{3}\pi$. The approximate solutions of (6.7) are linear combinations of the Airy functions

$$\zeta = \mathrm{Ai}\,(e^{\pm\frac{1}{3}i\pi}\sigma y), \tag{6.9}$$

the error being of order $|\sigma r_c|^{-1}$ when $|\sigma y|$ is of order unity. The approximation is valid for large $|\sigma r_c|$ provided that $|y/r_c| \ll 1$, so that S_3 can be defined as the range of real values of r that satisfy this relation. Such a range always exists if the imaginary part of r_c is small for large $|\mu r_c|$, which is true in all the cases considered later. In any case, the approximations are valid in the appropriate part of the complex r-plane. On the other hand, the upper 'end' of the range, S_2, of validity of (6.5) and the lower 'end' of the range, S_4, are both defined by $|\sigma y| \gg 1$. Thus the overlap range will be the part of the real axis in the overlap region

$$|\sigma|^{-1} \ll |y| \ll |r_c|$$

of the complex r-plane, which exists because $|\sigma r_c| = |2\mu^2 r_c^2|^{\frac{1}{3}}$ is large. Note, however, that the smallest value of $|\sigma r_c|$, that is, the value for the mode $m = 1$, is $2^{\frac{5}{3}}$ which is not particularly large, and so (6.9) is not such a good approximation for the first two or three m-modes, although it will be for all the other modes so far considered.

The stream function and velocity components corresponding to (6.9) can be found by integration, using (2.2) and (2.3). To the first order, these equations become, in S_3,

$$d\phi/dy = -r_c u, \quad du/dy = r_c\zeta.$$

The first equation may be integrated directly, using the second equation and (6.7) to give

$$\phi = -r_c y u + r_c^2\sigma^{-3}d\zeta/dy + B, \tag{6.10}$$

where B is a constant of integration. Then u can be found using the second equation together with (6.9), showing that the approximate expressions for u in S_3 involves integrals of Airy functions, but the coefficients involved can only be found by matching with (6.5) and (6.6). In the overlap region $|y/r_c|$ is small, and so (6.6) becomes

$$g \simeq K - \tfrac{2}{3}(\sigma y)^{\frac{3}{2}},$$

where

$$K = \mu\int_0^{r_c}(1-r^2/r_c^2)^{\frac{1}{2}}\,dr = \tfrac{1}{4}\pi\mu r_c, \tag{6.11}$$

while (6.5) shows that

$$u + \phi'/r \simeq i(\pi^{\frac{1}{2}} r_c \sigma^3)^{-1} (\sigma y)^{-\frac{3}{4}} [\exp\{i(K - \tfrac{3}{4}\pi - \tfrac{2}{3}(\sigma y)^{\frac{3}{2}})\} + \exp\{-i(K - \tfrac{3}{4}\pi - \tfrac{2}{3}(\sigma y)^{\frac{3}{2}})\}] + A\alpha I_0(\alpha r_c). \quad (6.12)$$

It can now be seen that the appropriate combination of integrals of the Airy functions (6.9) that give the velocity component u in S_3 is

$$u = -2(r_c \sigma^3)^{-1} \left[e^{iK} \int_\infty^{\exp(\frac{1}{3}i\pi)\sigma y} \mathrm{Ai}\,(t)\,dt + e^{-iK} \int_\infty^{\exp(-\frac{1}{3}i\pi)\sigma y} \mathrm{Ai}\,(t)\,dt \right] + A\alpha I_0(\alpha r_c), \quad (6.13)$$

because $|\sigma y|$ is large in the overlap region, and the behaviour of the expression in (6.13) for large $|\sigma y|$ is given by (6.12). Also, comparison of (6.5) and (6.10) in the overlap region gives

$$B = A r_c I_1(\alpha r_c). \quad (6.14)$$

It has been assumed here that $|\arg(\sigma y)| < \frac{2}{3}\pi$ in the overlap region with S_2, an assumption of this nature being necessary since for large $|\sigma y|$ the integrals in (6.13) can have different asymptotic expressions for different values of $\arg(\sigma y)$. It is known that the range of $\arg(\sigma y)$ chosen is the correct one for each mode in the limit as $\beta R \to \infty$, the limiting eigenfunctions and eigenvalues having been found in §§ 4 and 5, and that the values of $\arg(\sigma y)$ for the overlap region of S_3 with S_4 fall within the range $0 < \arg(\sigma y) < \frac{4}{3}\pi$. The procedure followed below is to find an eigenvalue equation based on the assumption that these ranges of $\arg(\sigma y)$ are appropriate for finite values of βR as well, and this eigenvalue equation is then used to find how the eigenvalues for each mode change as βR is decreased from the large values for which the eigenvalues are already known. During this process, the assumptions on $\arg(\sigma y)$ are continuously checked to ensure they are not violated.

The matching process for relating approximations valid in S_4 with those valid in S_3 is the same as the process for relating approximations valid in S_2 with those valid in S_3, the only difference being in the range of $\arg(\sigma y)$ involved. First, we re-write (6.13) using the identity

$$1 + \int_\infty^{-s} \mathrm{Ai}\,(t)\,dt + \int_\infty^{\exp(\frac{1}{3}i\pi)s} \mathrm{Ai}\,(t)\,dt + \int_\infty^{\exp(-\frac{1}{3}i\pi)s} \mathrm{Ai}\,(t)\,dt = 0, \quad (6.15)$$

which follows from integrating formula (30) of Miller (1946) from $x = 0$ to $x = -s$, and using the relation

$$\int_0^\infty \mathrm{Ai}\,(t)\,dt = \tfrac{1}{3}.$$

The new way of writing (6.13) is

$$u = -2(r_c \phi^3)^{-1} \left[(e^{iK} - e^{-iK}) \int_\infty^{\exp(-\frac{1}{3}i\pi)\sigma y} \mathrm{Ai}\,(t)\,dt + e^{iK} \int_\infty^{-\sigma y} \mathrm{Ai}\,(t)\,dt \right] + 2\sigma^{-3} r_c^{-1} e^{iK} + A\alpha I_0(\alpha r_c). \quad (6.16)$$

The approximation to the stream function valid in S_4 will have the same form as (6.5), the differences being in the coefficients and in that the Bessel function K_1

will be involved in the inviscid part as well as I_1. Using (6.10) and the asymptotic behaviour of (6.16) for large $|\sigma y|$ leads to the formula

$$\phi = r^{\frac{1}{2}}(2\pi\mu^2 h'^5)^{-\frac{1}{2}} e^{-\frac{1}{4}i\pi}[(e^{iK} - e^{-iK})\, e^{-ih} - i\, e^{i(K+h)}] + CrI_1(\alpha r) + DrK_1(\alpha r), \quad (6.17)$$

where

$$h = \mu \int_{r_c}^{r} (1 - r^2/r_c^2)^{\frac{1}{2}}\, dr = g - K, \quad (6.18)$$

and C and D are constants which are required by the matching process to satisfy

$$Cr_c I_1(\alpha r_c) + Dr_c K_1(\alpha r_c) = Ar_c I_1(\alpha r_c),$$
$$C\alpha r_c I_0(\alpha r_c) - D\alpha r_c K_0(\alpha r_c) = A\alpha r_c I_0(\alpha r_c) + 2\sigma^{-3} e^{iK}.$$

The first condition follows from matching stream functions and the second from matching axial velocity components. The omission made by Hopf (1914) and by Corcos & Sellars (1959) corresponds to neglecting the last term of the second equation, this term coming from the penultimate term in (6.16), and so from the first term in (6.15). Eliminating C from the above pair of equations gives

$$D = -2\sigma^{-3} e^{iK} I_1(\alpha r_c). \quad (6.19)$$

The approximate eigenvalue equation

The approximate eigenvalue equation follows from the boundary condition that the velocity vanishes at the wall, i.e.

$$\phi(1) = \phi'(1) = 0.$$

Using the expression (6.17) for ϕ, these conditions yield, on elimination of the undetermined constant C,

$$I_1(\alpha)\,(2\pi\mu^2 h_1^3)^{-\frac{1}{2}} e^{\frac{1}{4}i\pi}\,[(e^{iK} - e^{-iK})\, e^{-ih_1} + i\, e^{i(K+h_1)}]$$
$$= -D = 2\sigma^{-3} e^{iK} I_1(\alpha r_c), \quad (6.20)$$

by (6.19), h_1 being the value of h at $r = 1$.

As a check it can be shown that the eigenvalues already found satisfy this equation approximately. First, the inviscid solutions found at the beginning of § 3 satisfy the equation since $e^{iK} = 0$ in that case. For the 'viscous' modes, the eigenvalues are known in the limit as $\beta R \to \infty$ from the work of §§ 4 and 5.

(i) For the modes discussed in § 4, $r_c \to 0$ and $e^{ih_1} \to 0$ as $\beta R \to \infty$, so that (6.20) reduces to $\exp(2iK) = 1$, which is satisfied exactly by the eigenvalues found in § 4, as comparison of (4.2) with the definitions (6.2) and (6.11) shows. It seems rather fortuitous that the agreement is exact since, for instance, the mode $m = 1$ is the one for which the least agreement would be expected from the form of approximation used.

(ii) For the modes discussed in § 5, $r_c \to 1$ and $e^{-iK} \to 0$ as $\beta R \to \infty$, so by (6.18) and (5.3)

$$h_1 \approx \tfrac{2}{3} z_q^{\frac{3}{2}}$$

and so (6.20) reduces to (5.9). The roots (5.10) were found on EDSAC by Newton's method as a preliminary to the computation described below.

Now the eigenvalues for the viscous modes corresponding to finite values of βR depend also on the parameter R. For simplicity we will consider only the

limit for which $R = \infty$, so that in (6.20) $I_1(\alpha r_c)/I_1(\alpha)$ will be replaced by r_c, $|\alpha|$ being zero in this limit. For the limit to be a good approximation, β should be small, and in Leite's experiments β is always less than one, so that the limit is not unrealistic. The values of αR satisfying the equation were found by decreasing βR in steps from the large values for which αR is already known, and adjusting αR at each step in order to satisfy the equation. Checks were also made at each step to ensure that the conditions under which (6.20) is valid were not violated. The computer EDSAC was used for the purpose, and more details of the method are given in my thesis (Gill 1963). The results are shown in figure 5, the labels for large values of βR corresponding to the values of m and q introduced in §§ 4 and 5. As $\beta R \to 0$ it will be noticed that another limit is approached. For this limit $r_c \to 1$ and so (6.20) becomes approximately

$$\exp(2iK + 2ih_1) = i,$$

so that

$$K + h_1 = (l + 3/4)\pi,$$

where $l = 1, 2, 3, 4, \ldots$. As βR becomes smaller, h_1 eventually becomes so small that the boundary point $r = 1$ is very close to the critical point $r = r_c$ so that the approximation valid in S_3 must be used for application of the boundary conditions and determination of the eigenvalue equation instead of the approximation valid in S_4. Using (6.10) and (6.12), it is found that the appropriate equation is

$$e^{-2iK} = -\int_{\infty}^{\exp(\frac{1}{3}i\pi)\sigma y_1} \mathrm{Ai}(t)\,dt \Big/ \int_{\infty}^{\exp(-\frac{1}{3}i\pi)\sigma y_1} \mathrm{Ai}(t)\,dt,$$

where $y_1 = r_c - 1$. As $\beta R \to 0$, $y_1 \to 0$ and the right-hand side of the equation tends to -1. By (6.2) and (6.11), this implies that in the limit

$$\left.\begin{aligned} &\alpha_i R \approx (4l+2)^2, \\ &c = \beta/\alpha_r \approx \tfrac{1}{2} + 0{\cdot}6(2l+1)^{-\frac{1}{3}}. \end{aligned}\right\} \tag{6.21}$$

The exact limiting equation for $\beta R = 0$ is (6.1) with $r_c = 1$, and $u^2 = \alpha_i R$ playing the role of eigenvalue. The stream function satisfies (2.3). The first few modes can easily be found by expanding solutions in power series in r, for different values of μ, and thus finding the values of μ for which the boundary conditions are satisfied. The values for the first three modes were found in this way at the M.I.T. Computation Centre, the values being

$$\mu = (\alpha_i R)^{\frac{1}{2}} = 5{\cdot}664,\ 9{\cdot}783,\ 13{\cdot}83, \tag{6.22}$$

and it is seen that (6.21) provides quite a good approximation.

Discussion of the results shown in figure 5

(i) The number of modes: it will be recalled that the number of q- and m-modes is of order $(\beta R)^{\frac{1}{2}}$, and so is finite for any given βR and decreases as βR decreases. However, in figure 5 it is seen that as βR decreases, there is a change from the behaviour for large βR and as βR tends to zero, the limiting values given approximately by (6.21) are approached. For instance the modes corresponding to $q = 1, 2, 3, 4$ for large βR change over into the modes $l = 4, 12, 21, 31$, and the modes given by $m = 1, 2, 3, 4$ for large βR change into the modes given by

$l = 1, 2, 3, 5$ for βR small. Now for the limit used in finding the l-modes to be a good approximation, $|1 - r_c|$ must be small, where r_c is given by (3.2). By (6.21) this requires that $4l$ be large compared with $(\beta R)^{\frac{1}{2}}$ so that as βR decreases, more and more l-modes appear to replace the q- and m-modes that disappear—just as is found to happen in figure 5.

(ii) Some experimental results of Leite's are included in figure 5 for comparison. The points shown were deduced from figure 13 of Leite (1959) in which the experimenter presented his results in a timewise form. To make a proper comparison with the theory, however, one needs to compare other features of the disturbance such as disturbance velocity profiles, as was done in §§ 4 and 5.

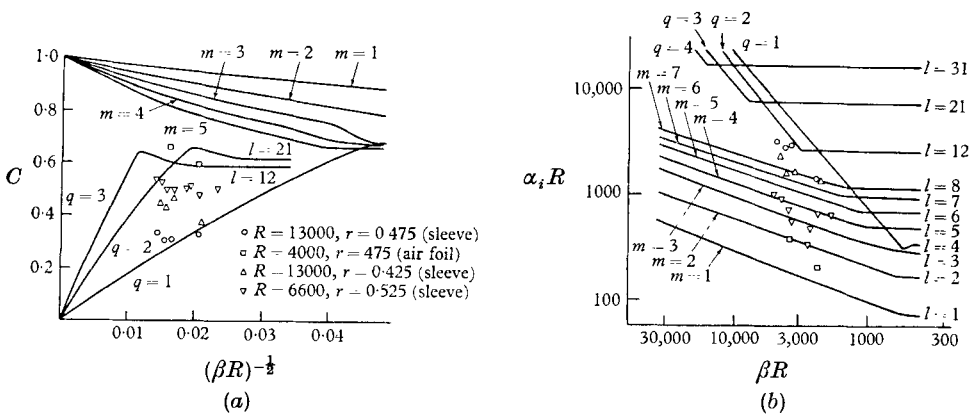

FIGURE 5. The change of (*a*) the non-dimensional wave-speed $c = \beta/\alpha_r$, and (*b*) the non-dimensional spatial damping rate, $\alpha_i R$, with the non-dimensional frequency $\beta R = 2\pi f a^2/\nu$ for various modes.

(iii) A significant feature of figure 5 is that damping rates decrease as the non-dimensional frequency βR decreases, the smallest damping rate being given by (6.22), that is

$$\alpha_i R \approx 32{\cdot}1.$$

Thus there is a zero-frequency disturbance whose amplitude does not fall to half its original amplitude until a distance of about $R/100$ diameters downstream of its source, that is a distance of about 10 diameters at a Reynolds number of 1000, and a distance of about 100 diameters at a Reynolds number of 10,000. Hence if the mean flow is distorted in some way at these high Reynolds numbers, it will stay distorted for a long distance downstream so that if the distorted profile is unstable, fluctuating disturbances will have a good chance to grow to a significant level before the mean flow becomes stable again. This seems to happen in some other experiments of Leite (1956) reported also by Kuethe (1956), in which disturbances to the flow in the pipe were produced by a circular airfoil. The Reynolds number of the flow was 12,000. From figure 2 of Kuethe's paper it is seen that the distortion of the mean flow from the Poiseuille profile remained at about the same amplitude for the first ten diameters, during which distance the fluctuating disturbance grew from a very small amplitude to an amplitude of the same order as the distortion of the mean flow. Beyond that point the flow changed in character and eventually approached a fully turbulent state.

This work was supported in part by the Office of Naval Research. Part of it was done while in the Department of Mathematics at the Massachusetts Institute of Technology.

REFERENCES

CORCOS, G. M. & SELLARS, J. R. 1959 *J. Fluid Mech.* **5**, 97.
EKMAN, V. W. 1910 *Arkiv. Mat. Astron. Fysik*, **6**.
ERDÉLYI, A. 1956 *Asymptotic Expansions*. New York: Dover.
GILL, A. E. 1962 *J. Fluid Mech.* **14**, 557.
GILL, A. E. 1963 Ph.D. Thesis, University of Cambridge.
GROHNE, D. 1954 *Z. ang. Math. Mech.* **34**, 344.
HOFF, L. 1914 *Ann. Physik*, **44**, 1.
KELVIN, LORD 1887 *Phil. Mag.* **24**, 188 (also *Math. and Phys. Papers*, **4**, 321).
KUETHE, A. M. 1956 *J. Aero. Sci.* **23**, 446.
LEITE, R. J. 1956 *Univ. Michigan Engng Coll. Rep.* IP-188.
LEITE, R. J. 1959 *J. Fluid Mech.* **5**, 81.
LIN, C. C. 1955 *The Theory of Hydrodynamic Stability*. Cambridge University Press.
MILLER, J. C. P. 1946 *Brit. Ass. Math. Tables*, pt. vol. B. Cambridge University Press.
PEKERIS, C. L. 1948 *Proc. U.S. Nat. Acad. Sci.* **34**, 285.
PRETSCH, J. 1941 *Z. ang. Math. Mech.* **21**, 204.
RAYLEIGH, LORD 1880 *Proc. London Math. Soc.* **11**, 57 (also *Sci. Papers*, **1**, 474).
RAYLEIGH, LORD 1892 *Phil. Mag.* **34**, 59 (also *Sci. Papers*, **3**, 575).
REYNOLDS, O. 1883 *Phil. Trans.* **174**, 935 (also *Sci. Papers*, **2**, 51).
RIIS, E. 1962 *Geof. Publ. Norske Vid. Akad., Oslo*, **23**, no. 4.
SCHENSTED, I. V. 1960 *Univ. Mich. Engng Coll. Tech. Rep.*
SEXL, T. 1927 *Ann. Phys., Lpz.*, **83**, 835; **84**, 807.
SEXL, T. & SPIELBERG, K. 1958 *Acta Phys. Austriaca*, **12**, 9.
WASOW, W. 1953 *J. Res. Nat. Bur. Stand.* **51**, 195.
WATSON, J. 1962 *J. Fluid Mech.* **14**, 211.
ZONDEK, B. & THOMAS, L. H. 1953 *Phys. Rev.* **90**, 738.